P-Type Doping Control of Magnetron Sputtered NiO for High Voltage UWBG Device Structures

Matthew A. Porter
Center for Power Electronics
Systems
Virginia Tech
Blacksburg, VA, USA
maporter@vt.edu

Yunwei Ma
Center for Power Electronics
Systems
Virginia Tech
Blacksburg, VA, USA
yunwei@vt.edu

Yuan Qin Center for Power Electronics Systems Virginia Tech Blacksburg, VA, USA yuanqin@vt.edu Yuhao Zhang Center for Power Electronics Systems Virginia Tech Blacksburg, VA yhzhang@vt.edu

Abstract—A major challenge in the design and fabrication of power devices from ultra-wide bandgap (UWBG) materials is the lack of a native shallow acceptor dopant for most materials in that class. P-type regions in UWBG devices may alternatively be formed by the deposition of p-type wide bandgap materials such as nickel oxide (NiO) to form heterojunctions. This work examines the effectiveness of the modulation of the acceptor concentration (NA) of magnetron sputtered NiO via the control of O2 partial pressure during sputtering. NiO/n+-Ga2O3 PN junctions are fabricated via sputtering using O2/Ar percentage ratios ranging from 0% to 12.5%. The acceptor doping and acceptor level characteristics are studied via the dependence of PN junction capacitance upon voltage, temperature and frequency. It is found that the N_A can be controlled between 9×10^{17} cm⁻³ at 0% O₂/Ar to 2×10¹⁸ cm⁻³ at 12.5% O₂/Ar partial pressure. Studies of the capacitance of the diodes shows that the associated first ionization level of the Ni³⁺ vacancy thought to be responsible for the p-type doping of the NiO is 0.35 eV, with suggestion of a second ionization level at 0.54 eV seen in the 0% O₂/Ar sample. To demonstrate the feasibility of utilizing magnetron sputtered NiO in power devices, a lateral RESURF terminated Ga₂O₃ Schottky diode is fabricated. Charge balance to maximize breakdown voltage is demonstrated in the Schottky diode as a function of NiO RESURF thickness, showing the viability of NiO in high voltage power devices for field spreading regions such as RESURF layers and JTE structures.

Keywords—power electronics, power semiconductor devices, nickel oxide, gallium oxide, wide-bandgap, ultra-wide bandgap

I. INTRODUCTION

Ultra-wide bandgap semiconductors (UWBGs) such as β-Ga₂O₃ and AlN are promising candidates for next generation power device designs, due to an increase in critical electric field and implied reduction in potential device losses [1]. However, hole transport and p-type doping in UWBG materials remains a major obstacle to their successful use in power device designs. For example, no native acceptor dopant is currently known for β-Ga₂O₃, and the self-trapping of holes limits hole transport in that material [2], [3]. Beyond the lack of native dopants, advanced power device designs require a method of selectivearea doping to create post-growth p-type regions in desired areas of the device [1]. Successful selective area p-type doping in many wide bandgap (WBG) and UWBG materials such as GaN via traditional methods such as implantation has been shown to be challenging [4], [5], requiring high N₂ overpressure or pulsed thermal annealing for acceptor activation [6].

This work is in part supported by National Science Foundation under Grants ECCS-2230412 and ECCS-2036915, Office of Naval Research monitored by Lynn Petersen (N00014-21-1-2183), and the Center for Power Electronics Systems Industry Consortium at Virginia Tech.

An alternative method of achieving effective selective-area p-type doping in UWBG power devices is through the deposition of WBG or UWBG materials which can be easily doped p-type. The transparent conductive oxide NiO is a naturally p-type material with a bandgap of 3.7 eV [3]. The native acceptor in NiO is believed to be due to Ni³⁺ charge states formed due to Ni vacancies in the material [7]. NiO deposited using conformal deposition techniques such as reactive magnetron sputtering and pulsed laser deposition has been demonstrated to maintain p-type conduction and doping after deposition [8]. In addition, high O₂ partial pressures during RF sputtering of NiO has been shown to modulate the effective hole density of the resulting NiO film [9], [10].

Recent work in incorporating NiO into power devices has been successful in using reactive magnetron sputtered NiO in β -Ga₂O₃ power PN diodes as both a junction termination extension (JTE) edge termination and hole injection layer, resulting in the achievement of breakdown voltages (V_{br}) of 2.5 kV with specific on-resistance (R_{on,sp}) of 5.9 m Ω .cm² [11]. Further work in [12] demonstrated avalanche capable NiO-Ga₂O₃ PN diodes with a V_{br} of 1.5 kV via an edge termination design using a combination of a high-k dielectric field plate and magnetron sputtered NiO JTE. NiO has also been utilized to form a charge-balance Ga₂O₃ with a V_{br} up to 10 kV and operational temperature of 200 °C [13]. In addition to forming planar PN junctions, NiO has also been used to form PN junction on 3D FinFET and trigate structures in GaN power devices [14]–[17].

This paper explores the variation of acceptor concentration (N_A) in reactive magnetron-sputtered NiO films via O₂ partial pressure control during the sputtering process. NiO films are deposited under varying O₂ partial pressure on a n⁺-Ga₂O₃ substrate to form p-NiO/n⁺-Ga₂O₃ diodes. The behavior of the capacitance of the fabricated diodes are studied as a function of voltage, frequency and temperature (C-V-T/f) to understand the dependence of the acceptor doping on O₂ partial pressure during sputtering, as well as the nature of the acceptor state giving rise to the doping. It is found that effective acceptor doping concentrations can be controlled between 9×10^{17} cm⁻³ to 2×10^{18} cm⁻³ utilizing the Ni³⁺ level believed to be responsible for the acceptor doping is a deep acceptor with ionization energy of 0.35 eV, with a second ionization level near 0.54 eV. Utilizing the studied NiO sputtering conditions, a p-NiO reduced-surfacefield (RESURF) terminated lateral Ga₂O₃ Schottky diode similar to the one in [13], [18], [19] is fabricated. Charge balance as a function of p-NiO RESURF thickness is successfully achieved,

demonstrating the potential for NiO as a p-type substitute for UWBG device applications.

II. DEVICE FABRICATION PROCESSES

A. P- NiO/n^+ - Ga_2O_3 Diode Fabrication

The p-NiO/n $^+$ -Ga $_2$ O $_3$ diode design used for the characterization of NiO was fabricated via reactive magnetron sputtering of NiO on an (001) n $^+$ -Ga $_2$ O $_3$ wafer with a doping level of 8.3×10^{18} cm $^{-3}$ grown by Novel Crystal Technologies. Fig. 1(b) illustrates the fabrication process for the device. Ti/Au backside cathode contacts are formed via e-beam deposition on the n $^+$ -Ga $_2$ O $_3$ wafer. p-NiO is then deposited via reactive magnetron sputtering. The sputtering process is described in more detail in Section III. Table 1 shows the four NiO sputtering conditions used to fabricate the diodes studied in this work. Recipe D (Ar/O2 partial pressure ratio of 2:1) is used to deposit a p $^+$ -NiO layer for ohmic contact after deposition of a p-NiO film using recipes A, B or C. Ni/Au anode contacts are deposited on the p $^+$ -NiO via e-beam deposition.

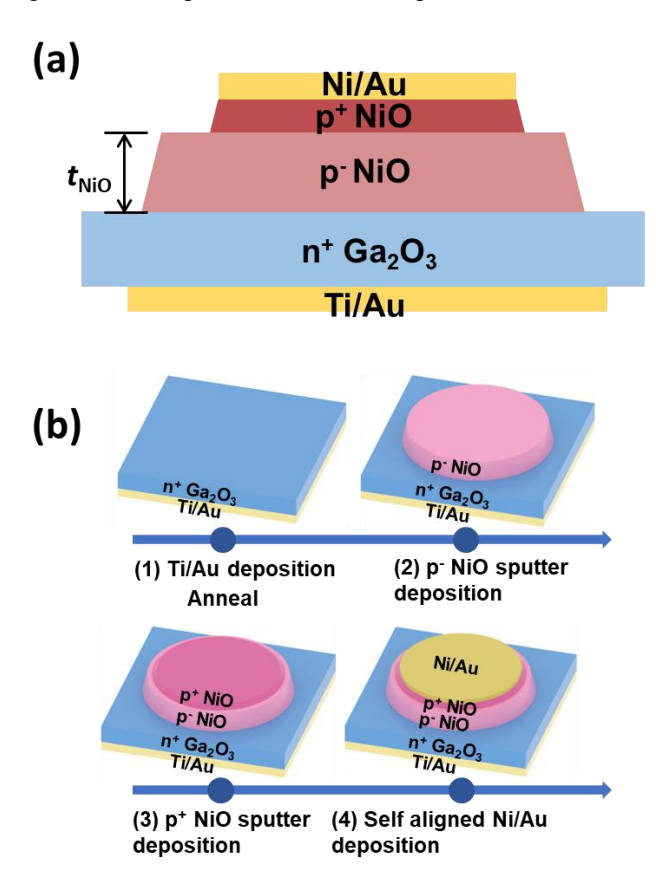


Fig. 1. P-NiO/n+Ga2O3 PN diode design and fabrication process. (a) illustrates the design of the diode, and (b) shows the fabrication process flow.

Table 1. NiO reactive magnetron sputtering conditions studied in this work.

Recipes	Ar flow (sccm)	O ₂ flow (sccm)	Rate (nm/Hour)	Resistivity $(\Omega \cdot m)$	H _D (nm)
Recipe A	60	0	49	84	147/340/540
Recipe B	58	3	21	6.9	63/147/244
Recipe C	54	6.8	24	0.53	48/95/156
Recipe D	40	20	20	1.8×10 ⁻³	N/A

B. P-NiO RESURF Terminated Lateral Ga₂O₃ Schottky Fabrication

The lateral Ga_2O_3 schottky diode used to study charge balance was fabricated on a Novel Crystal Technologies MBE-grown Ga_2O_3 n-/UID/n+ wafer. The doping level and thickness of the top n- channel layer were measured to be 2×10^{17} cm⁻³ over 70 nm via electrochemical C-V profiling. The UID layer was similarly measured to be doped at a concentration of 10^{16} cm⁻³ over 220 nm. Ni/Au Schottky contacts and Ti/Au ohmic contacts were formed via e-beam deposition at an anode-to-cathode separation of $17~\mu m$. RESURF termination of the diode was accomplished prior to Schottky contact deposition via reactive magnetron sputtering of NiO of varying thickness using recipes A and B from Table 1. The length of the NiO RESURF region was $10~\mu m$ for all diodes tested.

III. NIO ACCEPTOR CHARACTERIZATION

The PN diodes described in Section II were used to characterize the dependence of NiO acceptor concentration on sputtering conditions. Three lots of diodes were fabricated using NiO sputtered via recipes A, B and C. Thickness of the p-NiO film was 48 nm for recipe C, 244 nm for recipe B and 540 nm for recipe A (Table 1). A Kurt. J. Lesker Inc. PVD-75 RF magnetron sputtering chamber was used to deposit the NiO. 99.9% purity NiO sputtering targets supplied by Kurt J. Lesker Inc. were utilized as the source for deposition. Ar and O₂ plasma was used with a total chamber pressure of 3 mTorr and RF power of 100 W.

Characterization of the diodes was performed using a temperature-controlled probe station and a Keithley 4200 parameter analyzer. Initial characterization of the resistivity of the deposited NiO films was performed via TLM test structures fabricated alongside the diodes under test. Table 1 shows the variation of NiO sheet resistance with varying Ar/O₂ partial pressure ratio. Sheet resistance decreases from 84 Ω ·m to 0.53 Ω ·m as Ar/O₂ partial pressure ratio increases from 0% (recipe A) to 12.5% (recipe C). Accounting for film thickness, this decrease in sheet resistance suggests an increasing hole concentration in the NiO film with increasing O₂ pressure during deposition.

Figs. 2 (a-c) show the initial C-V characterization as a function of sputtering recipe and device temperature. C-V measurements were performed at a test frequency of 5 kHz. The $1/C^2$ characteristics of the measured C-V characteristics show good linearity over all temperatures, with an intercept of

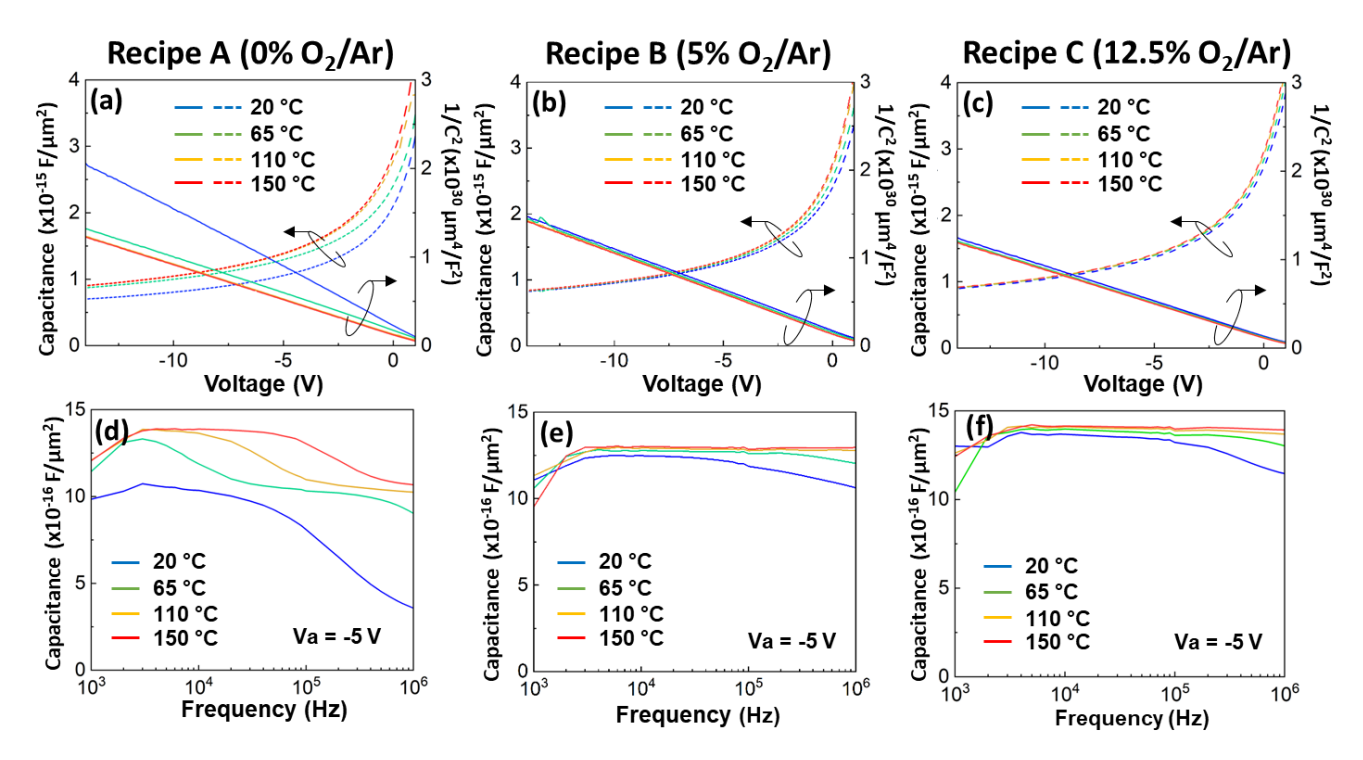


Fig. 2. C-V and C-f characterization of p-NiO/ n^+ -Ga₂O₃ diodes versus temperature and NiO sputtering conditions. (a-c) show the C-V characterization as a function of temperature, and (d-f) show the temperature dependence of capacitance dispersion at -5 V reverse bias.

1.7 V corresponding to the built-in voltage (V_{bi}) of the p-NiO/n⁺-Ga₂O₃ junction. However, a large temperature dependence of the capacitance characteristics is observed for the 0% Ar/O2 partial pressure sputtering condition (recipe A). The N_A of the p-NiO layer is extracted using the measured $1/C^2$ -V characteristics, correcting for the n⁺-Ga₂O₃ doping of 8.3×10^{18} cm⁻³ and assuming the relative permittivity of Ga₂O₃ and NiO to be 11.9 and 12.4, respectively [20][21]. The temperature dependence of the capacitance of the diode with NiO sputtered with a 0% Ar/O2 ratio (recipe A) resulted in a temperature dependent estimate of N_A . At 25 °C, the calculated doping of the 0% Ar/O2 NiO was 9.6×10^{17} cm⁻³ at 20 °C, and 1.58×10^{18} at 150 °C. The magnitude of N_A at 5 kHz of NiO sputtered with recipes B and C (5% and 12.5% O₂/Ar ratios) show little temperature dependence, and are calculated to be 1.5×10^{18} cm⁻³ and 1.9×10^{18} cm⁻³, respectively.

Figs. 2(d-f) show the measured C-f dispersion of the diodes as a function of sputtering recipe and device temperature at a reverse bias of -5 V. Frequency dispersion, with capacitance measured to decrease after an observed corner frequency, is found in diodes fabricated with NiO sputtered via all three recipes over the measured 5 kHz to 1 MHz range, with the most significant dispersion found in diodes sputtered with 0% O₂/Ar ratio (recipe A). For all recipes, the cutoff frequencies increase in magnitude as a function of temperature. For recipes B and C (5% and 12.5% O₂/Ar), the corner frequency moves beyond the measurable frequency range for temperatures greater than 65 °C. Two corner frequencies are visible in the C-f characteristics of the diodes with NiO sputtered with 0% Ar/O₂; both are visible

in the measured range at 65 °C and increase in magnitude with temperature.

The origin of the frequency dispersion in the measured C-f characteristics can be explained by a high activation energy of the acceptor level giving rise to the p-type doping in Ni-deficient NiO. To extract the acceptor activation energy, two methods were explored. TCAD simulation of the fabricated device structure was used to fit the measured C-f characteristics. Simulations were performed with an acceptor trap level giving rise to the p-type doping in the NiO layer. For the case of NiO deposited with 0% O₂/Ar (recipe A), two independent acceptor trap levels were assumed to achieve a good fit. Data fitting using the simulation output was used to extract the acceptor energy levels and doping concentrations necessary to fit the measured results.

Figs. 3 (a-c) show the results of the fitting of the simulation output to the measured C-f characteristics. The table in Fig. 3(d) shows the extracted acceptor characteristics from the fitting. For recipes B and C (5% and 12.5% O2/Ar), an acceptor ionization energy of 0.325 was found, and good agreement is found between the Na values obtained by the fit and the value extracted from C-V characterization at 5 kHz. For recipe A, the presence of two traps resulted in an extracted first acceptor ionization energy of 0.315 eV and second acceptor ionization energy of 0.44 eV. The acceptor ionization energy extracted for recipes B and C and the first ionization energy extracted for recipe A are close to value obtained via similar measurements on magnetron sputtered and PLD deposited NiO in [8], and are close to the

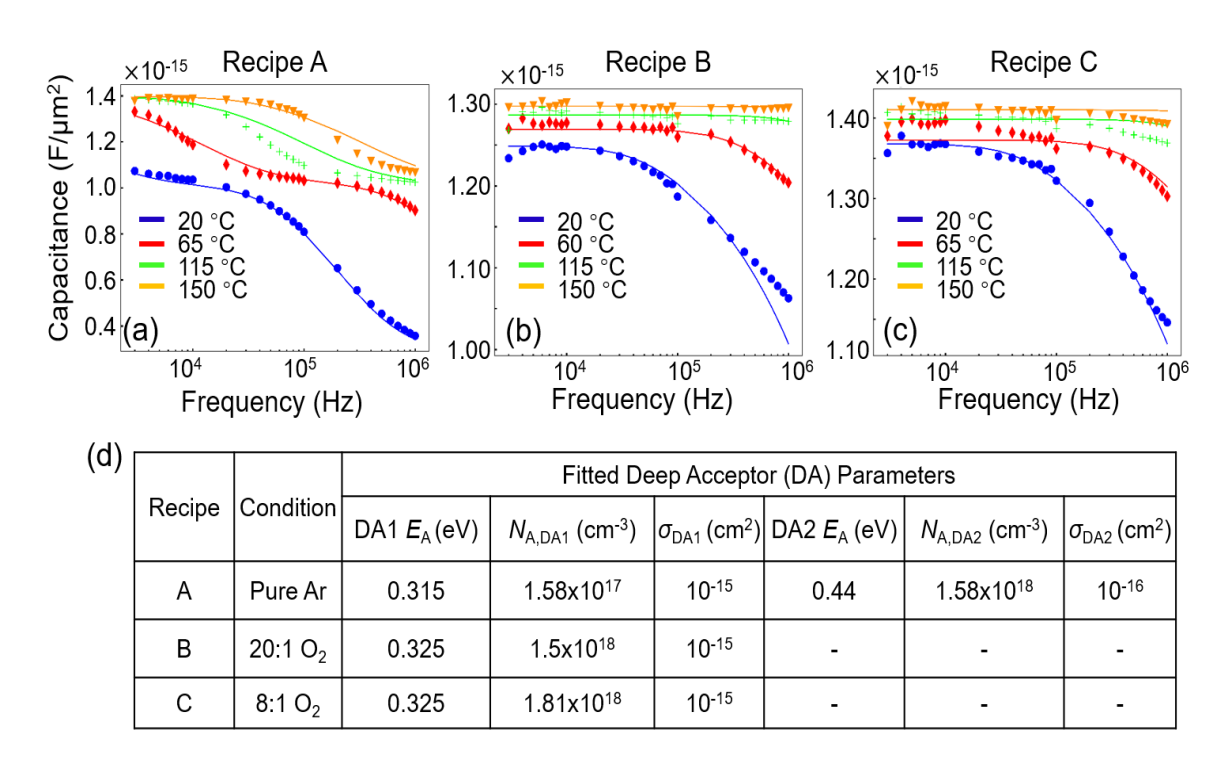


Fig. 3. Fitted capacitance-frequency dispersion of p-NiO/n⁺-Ga₂O₃ diodes at -5 V reverse bias versus temperature and sputtering conditions and TCAD extracted acceptor characteristics. (a-c) show the measured and fitted C-f dispersion characteristics as a function of temperature. The table in (d) shows the acceptor characteristics extracted via the TCAD fitting method.

theoretically expected value for the first ionization energy of the Ni³⁺ (0/-1) charge state associated with Ni vacancies in NiO. Similar theoretical calculations place the (-1/-2) Ni vacancy activation energy at 0.6 eV [22]. However, if the second acceptor energy extracted from the simulation is to be assigned to (-1/-2), then the extracted concentration of the second acceptor trap used to represent it should be twice that of the trap used to represent the (0/-1) transition. This discrepancy is a result of using multiple independent acceptor states to represent the varying charge state of a single physical acceptor, as the percentage of acceptors ionized in the (0/-1) and (-1/-2) states is dependent upon the local Fermi level and must sum to 100% [23].

To examine the nature of the acceptor level more closely in NiO films sputtered with 0% O₂/Ar partial pressure ratios, further measurements of the C-f dispersion at -5 V reverse bias were taken. Fig. 4 shows the results of C-f-T characterization of diodes fabricated with 0% O₂/Ar during NiO sputtering between 30 °C and 120 °C in 10 °C steps at -5V reverse bias. The temperature behavior of the first and second cutoff frequencies in the C-f dispersion can be clearly seen to be increasing. The acceptor activation energies are extracted from the dispersion measurements following the analysis of Schibli and Milnes for the C-f characteristics of a p-n⁺ junction doped with a deep acceptor [24]. If the p-type acceptor is a deep level, then the corner frequency in the dispersion characteristics can be shown to be related to the acceptor activation energy by

$$\frac{\omega_c}{T} \propto \exp\left(\frac{E_a - E_v}{kT}\right) \tag{1}$$

In Equation (1), ω_c is the corner frequency, Ea-Ev is the acceptor activation energy relative to the valence band edge and T the temperature. The intersection of the measured C-f characteristics as a function of temperature with a capacitance value chosen near the visible corner frequency in the plot was used to extract the corner frequency. It is assumed that the analysis in [24] continues to hold for acceptors with multiple Using Equation 1, the extracted corner charge states. frequencies can be plotted in an Arrhenius plot to determine the acceptor activation energies. Fig. 4 (b-c) shows the Arrhenius plot associated with the two observed corner frequencies in the C-f-T characteristics of recipe A diodes. A first activation energy of 0.35±0.03 eV is found for the corner frequencies associated with the dispersion region marked by ω_{T1} in Fig 4 (a), while an activation energy of 0.54±0.08 eV is found for the corner frequencies associate with the region marked by ω_{T2} . These values are close to the Ni^{3+} (0/-1) activation energy found experimentally in [8] and to the theoretical value for the (-1/-2) activation energy predicted in [22]. These experimentally extracted activation energies also support, within the error of the measurement, the values found via the TCAD fitting method.

Both the experimentally extracted and TCAD fitted activation energies found allow us to conclude that the Ni^{3+} acceptor can become doubly ionized in sputtered NiO films using the Ni vacancy as the acceptor level. The band diagram shown in Fig. 4(d) illustrates the origin and consequences of this double ionization. Given that the Ni^{3+} can transition from a charge state of -1 to a charge state of -2, the depletion region in the NiO will contain two regions of charge: one with magnitude -qN_A, and another with charge -2q(N_A), the extent of which depends upon the positions $W_{d,\mathrm{A1}}$ and $W_{d,\mathrm{A2}}$ where the hole

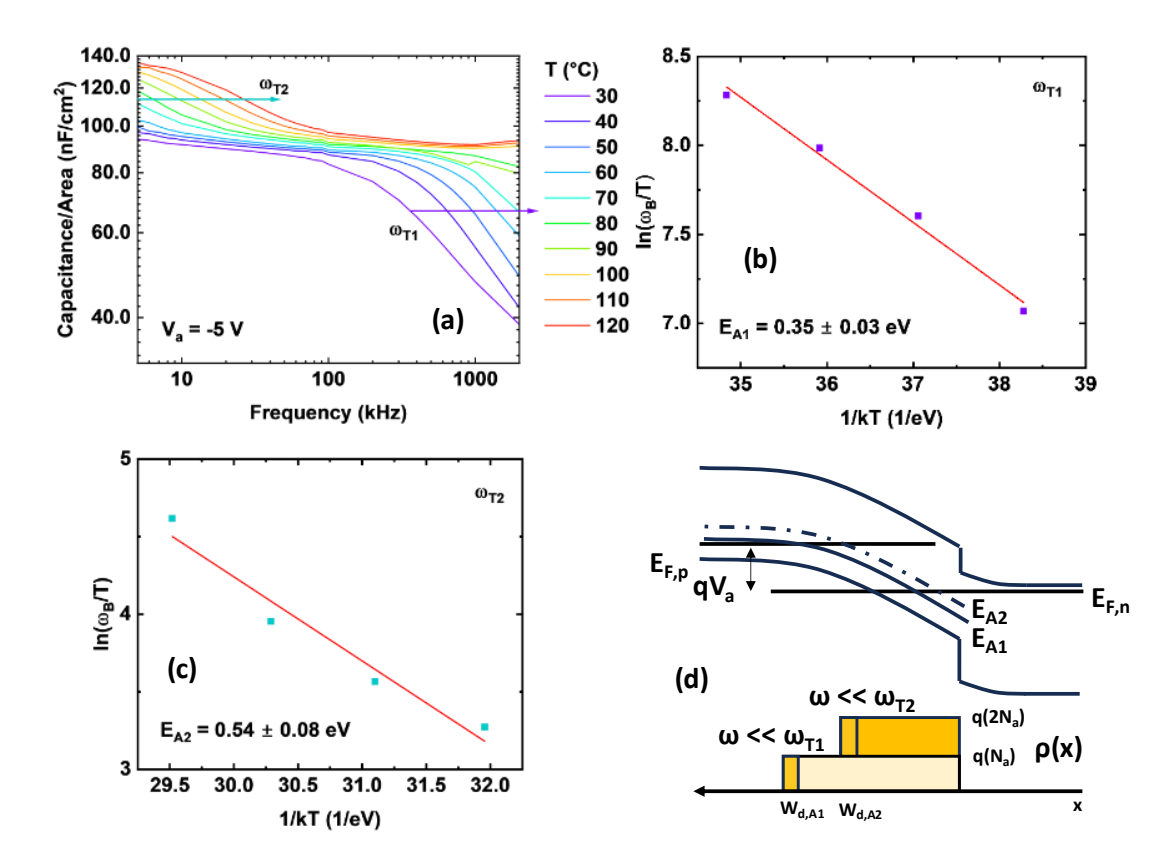


Fig. 4. Capacitance frequency dispersion at -5 V reverse bias for diodes fabricated with 0% O₂/Ar NiO. (b-c) show the extracted acceptor activation energies. (d) gives the band diagram for a p-NiO/n⁺-Ga₂O₃ PN diode with the assumed energy levels, as well as the charge distribution in the depletion width.

quasi-Fermi level crosses the associated activation levels with the (0/-1) and (-1/-2) charge transitions. At low frequency, acceptors at the band edge can make the (0/-1) charge transition, and acceptors near the point at which the hole quasi-fermi level crosses the second ionization energy can make also make the (-1/-2) charge transition, with both contributing to the measured capacitance. As frequency increases, only the acceptors at the depletion region edge can make the (0/-1) charge transition under the AC perturbation, reducing the capacitance. At high enough frequency, the charge state of the deep acceptor cannot follow the applied AC bias, resulting in highly reduced capacitance. This result suggests that the physical acceptor concentration in Ni vacancy doped NiO can be extracted from PN C-V measurements at a frequency low enough such that only the singly ionized acceptors at the edge of the depletion region can respond to the AC perturbation, but not low enough such that the (-1/-2) level can respond.

IV. CHARGE BALANCE IN NIO RESURF TERMINATIONS

Using the O₂/Ar sputtering conditions studied in Section III, reactive-magnetron sputtered NiO was used in a lateral RESURF Ga₂O₃ Schottky diode to demonstrate the viability of the material in power device applications. Lateral Schottky diodes with magnetron sputtered NiO p-type RESURF terminations were fabricated as described in Section II.B. The RESURF termination will maximize the measured breakdown

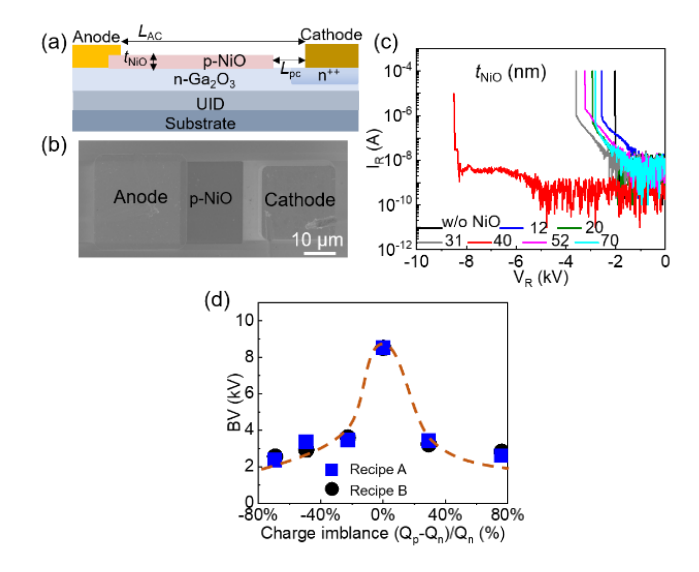


Fig. 5. p-NiO RESURF Ga₂O₃ Schottky diode device structure and breakdown voltage measurements as a function of NiO thickness. (a) and (b) show the device structure, (c) shows the measured breakdown as a function of NiO thickness for recipe A, and (d) plots Vbr vs. charge balance for both recipes.

voltage through the charge balance condition $\sigma_n L_{ac} = (L_{ac} - L_{pc}) t_{NiO} N_A$, where σ_n is the total doping dose of the n+ Ga_2O_3 channel, measured at 3.8×10^{12} cm $^{-2}$ by electrochemical C-V profiling, L_{ac} is the anode-to-cathode separation of 17 um, and L_{pc} is the cathode-to-RESURF separation of 7 um. Recipes A and B (0% and 5% $O_2/Ar)$ were used to deposit NiO RESURF layers of thickness varying between 12 nm and 70 nm for charge balance testing.

Fig. 5 shows the device structure, breakdown voltage measurements as a function of NiO thickness and temperature and breakdown voltage as a function of estimated charge imbalance. Diodes using a 0% O₂/Ar NiO RESURF layer reach an optimal breakdown voltage of 8 kV at a NiO thickness of 75 nm, while diodes using a 5% O₂/Ar NiO RESURF layer reach an optimum breakdown voltage of also around 8 kV at a NiO thickness of 40 nm. Based upon the charge balance condition at the optimum breakdown design, the estimated N_A value of the 0% O₂/Ar NiO RESURF film is 8.6×10^{17} cm⁻³ while the estimated N_A of the 5% O₂/Ar NiO RESURF film is 1.6×10^{18} cm⁻³. These results successfully demonstrate the feasibility of using reactive-magnetron sputtered NiO as a selective-area ptype dopant for an UWBG power device.

V. CONCLUSION

This work examines the effect of varying O₂ partial pressure during sputtering of NiO thin films. Through capacitance measurements on p-NiO/n+-Ga2O3 diodes fabricated via magnetron sputtering, we have shown that the effective acceptor density in NiO deposited in this manner can be controlled from a magnitude of ~9×10¹⁷ cm⁻³ to 2×10¹⁸ cm⁻³ over an O₂/Ar partial pressure ratio range from 0% to 12.5%. Acceptor first and second ionization energies of 0.35 and 0.54 eV are extracted using the temperature dependent C-f dispersion of the fabricated diodes,, showing experimentally that the second charge state of the Ni³⁺ may occur in NiO films deposited via sputtering in the pure Ar atmosphere. A magnetron-sputtered NiO layer is used to successfully demonstrate charge balance in a lateral Ga₂O₃ Schottky diode, demonstrating the feasibility of the utilization of NiO for selective area doping in UWBG power devices. Further studies on the control of p-type doping in PLD deposited and Li-doped Ni films should be examined to further the understanding of the control of p-type doping in NiO for use in power device applications.

ACKNOWLEDGMENT

The authors thank the assistance and advice of Dr. Ming Xiao, Boyan Wang, Yifan Wang and Donald Leber at Virginia Tech, Joseph Spencer at NRL and Zhonghao Du at USC in assisting with device fabrication and technical support, as well as the collaboration with Silvaco on device simulation of our device structures.

REFERENCES

- [1] Y. Zhang, F. Udrea, and H. Wang, "Multidimensional device architectures for efficient power electronics," *Nat Electron*, vol. 5, no. 11, Art. no. 11, Nov. 2022, doi: 10.1038/s41928-022-00860-5.
- [2] J. L. Lyons, "A survey of acceptor dopants for β-Ga2O3," Semicond. Sci. Technol., vol. 33, no. 5, p. 05LT02, Apr. 2018, doi: 10.1088/1361-6641/aaba98.
- [3] J. A. Spencer, A. L. Mock, A. G. Jacobs, M. Schubert, Y. Zhang, and M. J. Tadjer, "A review of band structure and material properties of transparent conducting and semiconducting oxides: Ga₂ O₃, Al₂ O₃, In₂ O₃, ZnO, SnO₂, CdO, NiO, CuO, and Sc₂ O₃," Applied Physics Reviews, vol. 9, no. 1, p. 011315, Mar. 2022, doi: 10.1063/5.0078037.
- [4] Y. Zhang et al., "Vertical GaN Junction Barrier Schottky Rectifiers by Selective Ion Implantation," *IEEE Electron Device Letters*, vol. 38, no. 8, pp. 1097–1100, Aug. 2017, doi: 10.1109/LED.2017.2720689.
- [5] Y. Zhang and T. Palacios, "(Ultra)Wide-Bandgap Vertical Power FinFETs," *IEEE Transactions on Electron Devices*, vol. 67, no. 10, pp. 3960–3971, Oct. 2020, doi: 10.1109/TED.2020.3002880.
- [6] J. D. Greenlee, B. N. Feigelson, T. J. Anderson, J. K. Hite, K. D. Hobart, and F. J. Kub, "Symmetric Multicycle Rapid Thermal Annealing: Enhanced Activation of Implanted Dopants in GaN," ECS J. Solid State Sci. Technol., vol. 4, no. 9, p. P382, Aug. 2015, doi: 10.1149/2.0191509jss.
- [7] R. Karsthof, A. M. Anton, F. Kremer, and M. Grundmann, "Nickel vacancy acceptor in nickel oxide: Doping beyond thermodynamic equilibrium," *Phys. Rev. Mater.*, vol. 4, no. 3, p. 034601, Mar. 2020, doi: 10.1103/PhysRevMaterials.4.034601.
- [8] R. Karsthof, H. von Wenckstern, V. S. Olsen, and M. Grundmann, "Identification of LiNi and VNi acceptor levels in doped nickel oxide," APL Materials, vol. 8, no. 12, p. 121106, Dec. 2020, doi: 10.1063/5.0032102.
- [9] M. Xiao et al., "First Demonstration of Vertical Superjunction Diode in GaN," in 2022 International Electron Devices Meeting (IEDM), Dec. 2022, p. 35.6.1-35.6.4. doi: 10.1109/IEDM45625.2022.10019405.
- [10] X. Yin, Y. Guo, H. Xie, W. Que, and L. B. Kong, "Nickel Oxide as Efficient Hole Transport Materials for Perovskite Solar Cells," *Solar RRL*, vol. 3, no. 5, p. 1900001, 2019, doi: 10.1002/solr.201900001.
- [11] B. Wang et al., "2.5 kV Vertical Ga2O3 Schottky Rectifier With Graded Junction Termination Extension," *IEEE Electron Device Letters*, vol. 44, no. 2, pp. 221–224, Feb. 2023, doi: 10.1109/LED.2022.3229222.
- [12] F. Zhou et al., "An avalanche-and-surge robust ultrawide-bandgap heterojunction for power electronics," Nat Commun, vol. 14, no. 1, Art. no. 1, Jul. 2023, doi: 10.1038/s41467-023-40194-0.
- [13] Y. Qin et al., "10-kV Ga2O3 Charge-Balance Schottky Rectifier Operational at 200 °C," IEEE Electron Device Letters, vol. 44, no. 8, pp. 1268–1271, Aug. 2023, doi: 10.1109/LED.2023.3287887.
- [14] Y. Ma et al., "Tri-gate GaN junction HEMT," Appl. Phys. Lett., vol. 117, no. 14, p. 143506, Oct. 2020, doi: 10.1063/5.0025351.
- [15] Y. Ma, M. Xiao, Z. Du, H. Wang, and Y. Zhang, "Tri-Gate GaN Junction HEMTs: Physics and Performance Space," *IEEE Transactions on Electron Devices*, vol. 68, no. 10, pp. 4854–4861, Oct. 2021, doi: 10.1109/TED.2021.3103157.
- [16] M. Xiao et al., "5 kV Multi-Channel AlGaN/GaN Power Schottky Barrier Diodes with Junction-Fin-Anode," in 2020 IEEE International Electron Devices Meeting (IEDM), Dec. 2020, p. 5.4.1-5.4.4. doi: 10.1109/IEDM13553.2020.9372025.
- [17] Y. Zhang et al., "GaN FinFETs and trigate devices for power and RF applications: review and perspective," Semicond. Sci. Technol., vol. 36, no. 5, p. 054001, Mar. 2021, doi: 10.1088/1361-6641/abde17.
- [18] M. Xiao, Y. Ma, K. Liu, K. Cheng, and Y. Zhang, "10 kV, 39 mΩ·cm2 Multi-Channel AlGaN/GaN Schottky Barrier Diodes," *IEEE Electron Device Letters*, vol. 42, no. 6, pp. 808–811, Jun. 2021, doi: 10.1109/LED.2021.3076802.
- [19] M. Xiao et al., "Multi-Channel Monolithic-Cascode HEMT (MC2-HEMT): A New GaN Power Switch up to 10 kV," in 2021 IEEE International Electron Devices Meeting (IEDM), Dec. 2021, p. 5.5.1-5.5.4. doi: 10.1109/IEDM19574.2021.9720714.

- [20] K. V. Rao and A. Smakula, "Dielectric Properties of Cobalt Oxide, Nickel Oxide, and Their Mixed Crystals," *Journal of Applied Physics*, vol. 36, no. 6, pp. 2031–2038, Jul. 2004, doi: 10.1063/1.1714397.
- [21] A. Fiedler, R. Schewski, Z. Galazka, and K. Irmscher, "Static Dielectric Constant of β-Ga2O3 Perpendicular to the Principal Planes (100), (010), and (001)," ECS J. Solid State Sci. Technol., vol. 8, no. 7, p. Q3083, Mar. 2019, doi: 10.1149/2.0201907jss.
- [22] H. D. Lee, B. Magyari-Köpe, and Y. Nishi, "Model of metallic filament formation and rupture in NiO for unipolar switching," *Phys. Rev. B*, vol. 81, no. 19, p. 193202, May 2010, doi: 10.1103/PhysRevB.81.193202.
- [23] Milnes, A.G., Deep Impurities in Semiconductors. New York: John Wiley & Sons, Ltd, 1973.
- [24] E. Schibli and A. G. Milnes, "Effects of deep impurities on n+p junction reverse-biased small-signal capacitance," *Solid-State Electronics*, vol. 11, no. 3, pp. 323–334, Mar. 1968, doi: 10.1016/0038-1101(68)90044-